Available online at www.sciencedirect.com

ScienceDirect

Scripta Materialia 76 (2014) 81–84

Scripta MATERIALIA

www.elsevier.com/locate/scriptamat

Grain boundary misorientation dependence of β phase precipitation in an Al–Mg alloy

D. Scotto D'Antuono,[a] J. Gaies,[b] W. Golumbfskie[b] and M.L. Taheri[a,*]

[a]*Department of Materials Science and Engineering, Drexel University, Philadelphia, PA, USA*
[b]*Naval Surface Warfare Center, Carderock Division, West Bethesda, MD, USA*

Received 9 November 2013; revised 30 December 2013; accepted 3 January 2014
Available online 9 January 2014

Precipitation of β phase (Al3Mg2) in an Al–Mg alloy is investigated by in situ heating and precession diffraction-based orientation imaging in a transmission electron microscope. Initial β formation occurs more readily at low-angle grain boundaries than at high-angle boundaries; however, larger precipitates are found at high-angle boundaries. We propose a mechanism for β formation based on boundary energy and grain boundary free volume. These results advance the understanding of β phase formation, aiding future corrosion prevention.
© 2014 Acta Materialia Inc. Published by Elsevier Ltd. All rights reserved.

Keywords: Sensitization; In situ TEM; Misorientation; Aluminum alloy; β Phase

The Al–Mg 5xxx series aluminum alloy is a material commonly used in marine environments, such as naval ships and commercial vessels [1–3], and gains its strength from additions of >3% Mg and cold work, yielding medium strength and high ductility [2]. The use of Al5xxx instead of steel alloys allows for lighter ships with greater maneuverability and fuel efficiency; the use of aluminum can reduce ship weight by up to 22% [3]. A drawback of the use of the Al5xxx series alloy series, however, is its susceptibility to corrosion and cracking due to low-temperature sensitization [4,5].

Corrosion in Al5xxx results from sensitization, a process where the material is exposed to elevated temperatures from 50 to 400 °C for extended periods of time [6,7]. This phenomenon is characterized by the nucleation and growth of Al_3Mg_2 (β) precipitates, which can form along grain boundaries [8,9], and ultimately lead to stress corrosion cracking [9–12]. While the nucleation and growth mechanisms of the β phase are still not fully understood, it has been suggested that equilibrium β forms by the following reaction [4]:

$$\text{Solid solution}\,\alpha \rightarrow \text{GP zones} \rightarrow \beta'' \rightarrow \beta' \rightarrow \beta \qquad (1)$$

Note that GP zones and β″ have only been known to form in materials with >13% Mg.

The β′ precipitates are a metastable phase with a hexagonal crystal structure, semi-coherent to the matrix, typically forming between 50 and 200 °C [5]. The equilibrium β phase is cubic and incoherent with respect to the grain boundary nucleation sites. Due to the complexity of formation, the focus of this study will be on the formation of the final β phase at equilibrium.

While a wealth of evidence exists that β phase precipitation is a thermally activated process [13,14] occurring after long periods of exposure to temperature, little information exists on the early stages of its formation. Most observations of β phase growth concentrate on long-term precipitation studies over many hours of exposure to elevated temperatures (~50–150 °C) [15–17], originally performed to mimic ship exposure times [18]. Accelerated sensitization studies, which allow for the examination of earlier stages of β phase growth, are performed within temperature ranges of 150–175 °C for one to tens of hours [5,19]. Within this time and temperature regime, β phase precipitates have been observed to grow heterogeneously on grain boundaries and intermetallic precipitates [20,21]. Studies by Yassar et al. [4] and Goswami and Holtz [22] have suggested that initial β phase formation is facilitated by pipe diffusion of Mg via dislocations to the grain boundaries and that initial β phase growth appeared as isolated precipitates but, after long heat treatments, took on a ribbon-like morphology along grain boundaries. While these observations of pipe diffusion are valid [14] and assist in our understanding of how

* Corresponding author. Tel.: +1 2158956618; e-mail: mtaheri@coe.drexel.edu

1359-6462/$ - see front matter © 2014 Acta Materialia Inc. Published by Elsevier Ltd. All rights reserved.
http://dx.doi.org/10.1016/j.scriptamat.2014.01.003

β phase forms in Al5xxx alloys, they do not explain the anisotropy with respect to grain boundary type.

There exists a limited amount of information about the dependence of β precipitation on grain boundary character in 5xxx alloys [23,24]. Transmission electron microscopy (TEM)-based studies by Carroll et al. [9] characterized the effect of Zn additions on grain boundary precipitation in AA5083 after sensitization at 200 °C for 24 h. Their results revealed that β phase preferred both high-angle and subgrain boundaries; however, misorientation angle dependence was not examined. Unwin and Nicholson [25] compared Al–6Zn–3Mg and Al–7Mg aged for 3 h at 180 °C, and found that the Zn addition promoted nucleation at subgrains. They also found that precipitation was more difficult on low-angle than on random high-angle grain boundaries [25]. A recent study by Tan and Allen [26] observed the relationship between thermomechanical processing and the corrosion of AA5083, and revealed that samples with larger dislocation networks and low-angle grain boundaries exhibited superior corrosion resistance. This was consistent with a study by Davenport et al. [27], in which an examination AA5182 sensitized at 150 °C for 10 h using atomic force microscopy, electron back scattered diffraction and TEM showed that there was no sign of β phase on low-angle grain boundaries and that those with less than 20° misorientation are resistant to corrosive attack.

The general trend among these previous studies is that low-angle boundaries (<20° misorientation) in 5xxx alloys are resistant to corrosive attack due to precipitation occurring primarily on high-angle grain boundaries, free dislocations and intermetallic precipitates. The eventual formation of β on the above-mentioned microstructural features is clearly documented; however, there is still little evidence of their primary formation. A more predictive understanding of the initial nucleation mechanisms and growth of β phase in Al5xxx alloys is necessary. Using a coupled approach of in situ annealing and orientation imaging (Nanomegas ASTAR™) in a transmission electron microscope [28,29], the nucleation and growth of the β precipitates during sensitization is studied as a function of grain boundary misorientation.

Aluminum alloy 5456 (5.5%Mg), in the H116 temper condition, was prepared for in situ TEM from bulk as-received material using traditional metallographic polishing, and TEM preparation using a Fishione ion mill for final electron transparency. In situ sensitization was conducted using a Gatan heating holder; the temperature was ramped from room temperature to 300 °C at a rate of 0.3 °C s^{-1}, held at 300 °C temperature for 5 min, then reduced back down to room temperature. The temperature of 300 °C was chosen to accelerate β phase growth, which normally forms comparable precipitate sizes over 100 h of sensitization at 150 °C [5,27,30]. This temperature regime has been shown in previous studies [31,32] to yield β phase precipitates after 10 min, which is a reasonable time-frame for TEM studies. Post-heating analysis was conducted using the Nanomegas ASTAR™ system, which utilizes precession diffraction to match acquired TEM diffraction images to known diffraction patterns, with a precession angle of 0.60° at 100 Hz. Orientation maps were generated from nanobeam diffraction patterns acquired by the Nanomegas system by automated diffraction via beam rastering as well as manual nanobeam diffraction; energy-dispersive spectroscopic analysis was coupled with these techniques to reduce any ambiguity (see Supplementary Material). The experiments were repeated several times and yielded a total of 42 analyzed grain boundaries.

Bright-field TEM images of the unsensitized state of the material (before in situ sensitization) revealed an extensive subgrain structure and a high dislocation density, most likely due to the cold work from the H116 treatment. The H116 naming convention explains that the material is in a strain-hardened condition (the strain is between $^1/_8$ and $^1/_4$ of the fully hardened condition, in this case 12% rolling reduction) without a subsequent heat treatment [33]. The as-received condition also contained sparse amounts of pre-existing β′ precipitates, found on low-angle grain boundaries, which can also be attributed the final heat treatment of the H116 temper (Figs. 1(A) and 2(A)).

Areas containing previously existing β′ precipitates in the as-received material were chosen as the first sites for in situ observation due to a previous understanding that Mg-enriched, β′-containing areas lead to the formation of β in equilibrium [24,31]. Thus, before an extensive grain boundary dependency study could be performed, the dependence on previously existing β′ had to be examined as a baseline. In situ accelerated sensitization revealed that β′ precipitates began to dissolve at ~200 °C and were fully dissolved at ~275 °C, as shown in Figure 1. Equilibrium β first appears to nucleate at 275 °C, accompanied by a sharp change in contrast during in situ capture (Fig. 1C and D). During the experiments, new β′ precipitates did not form under these conditions, which could be attributed to the accelerated time of the annealing/sensitization.

The in situ heating experiments showed that pre-existing location of the β′ did not necessarily yield β phase, as shown in Figure 2B. The β′ dissolves before β forms. However, the location of the β nucleation was not observed to be correlated with the previous location of β′. The β′ does not transform into the cubic β and they do not share a common nucleation site. This agrees with previous findings during non-isothermal aging, when β′ and β dissolve and form independently of one another [34,35]. Extensive post-heating TEM analysis confirmed this observation (Fig. 2).

While the presence of β′ precipitates was determined to be a less significant factor in the nucleation and growth of β precipitates, a clear trend based on grain boundary type emerged: while higher-angle grain boundaries allowed for larger precipitate growth during in situ studies, precipitate nucleation occurred on low-angle grain boundaries as well, though accompanied by stagnated growth. To analyze this developing trend more quantitatively, post-sensitization analysis of the grown β precipitates was conducted using Nanomegas ASTAR™ orientation imaging in a transmission electron microscope to obtain orientation image maps of the annealed/sensitized microstructures. Specifically, TEM-based orientation imaging was used in conjunction with in situ and ex situ TEM analysis of β precipitation (see Fig. 3 and Supplementary Materials S1 and S2). Such analysis was performed on various heat-treated samples to yield the misorientation and

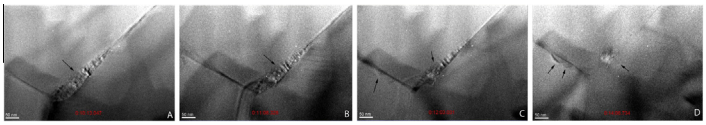

Figure 1. (A–D) Images taken in situ during the ramping of temperature from 200 to 300 °C. (A) Sample at 200 °C with pre-existing β′ precipitate. (B) Sample at 252 °C with β′ partially dissolved. (C) Sample at 275 °C with β′ dissolving and formation of β on left adjacent boundary. (D) Sample at 300 °C with some remaining β′ and β formation.

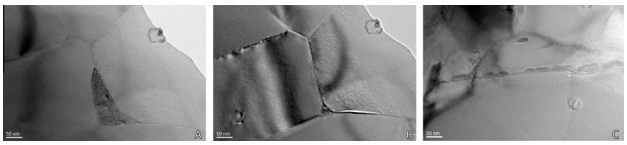

Figure 2. (A) Pre-existing β′ precipitate at the grain boundary before in situ heat treatment. (B) Dissolved β′ precipitate after 300 °C in situ heat treatment with no β formation. (C) Examples of β at locations close to but not at dissolved β′ precipitate.

precipitate size for 42 grain precipitate/grain boundary pairs (Fig. 3). The results suggest that more β phase was found at low-angle grain boundaries.

The plot in Figure 3 shows a comparison of grain boundary misorientation angles measured vs. precipitate size. The orientation scans were taken from various locations across a group of samples (with the same heat-treatment) to achieve more informed statistical information. Grain boundaries with misorientations from 15 to 40° appear to have no precipitates, but this can be attributed to the number of boundaries surveyed. It is believed that the precipitates occurred on all types of angles, but the random selection of areas observed did not contain those angles; however, the orientation maps show that the majority of precipitates during the in situ experiments are on low-angle (<15°) grain boundaries and dislocations (omitted in the plot). Another possible explanation for the clustering found at higher angles (Fig. 3) may be related to preferential precipitate growth at boundaries with sigma configurations such as $\sum 7$ or $\sum 9$, which are ~38° about the ⟨111⟩ and ⟨110⟩ axes, respectively [36] (as opposed to random high angles), but this would require further analysis. It should be noted that the precipitates on the low- and high-angle boundaries were observed over the entirety of the sample in thicker areas away from the center, or thinnest region, of the foil. Since precipitates of similar morphology, size and gain boundary angle (low and high) are observed away from the center, it can be concluded that the surface effect is not the primary precipitation mechanism [37,38]. Relatively few precipitates were seen to form on high-angle grain boundaries, but they were larger than those found on low-angle boundaries (indicating uninhibited growth).

The precipitate size increased with misorientation angle. Figure 4(B) and (C) shows a comparison between precipitates on a 5° low-angle boundary and a 40° high-angle boundary. Nucleation beading on very low angles (<3°) suggests that initial formation may occur on the low-angle substructure via dislocations (Fig. 4D), but is halted while uninhibited precipitate growth occurs on higher energy boundaries. Grain boundaries >15° are considered to be of low energy and thus are less attractive sites for nucleation when compared to higher-angle boundaries.

In this system the largest area observed on low-angle grain boundaries was around 4000 nm^2, but the majority of precipitates analyzed were closer to 2000 nm^2. Precipitates on high-angle grain boundaries, while more scarce, were triple the size of those on low-angle boundaries. This suggests that there is a size limitation of the β phase on the lower-energy low-angle grain boundaries. In some cases precipitates grew preferentially on the low-angle boundary despite being located only a few nanometers away from a high-angle grain boundary, in direct contrast to previous findings of high-angle grain boundary preference [28]. However, heat treatments [1] have been implemented previously to improve corrosion resistance in 5xxx alloys by increasing β precipitation at low-angle boundaries and within grains rather than at high angles. Thermomechanical processing is also being used to change the grain boundary distribution to mitigate corrosion [26], though the work in this area is still ongoing.

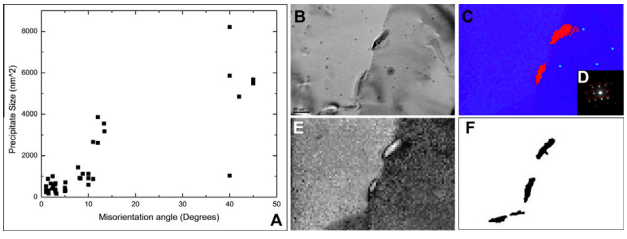

Figure 3. Plot of precipitate size vs. misorientation angle (A). Precipitate size analysis (B–F) TEM bright-field area of interest. (B) Nanomegas ASTAR™ orientation map; (C) diffraction pattern from the top precipitate; (D) pseudo-dark-field image from Nanomegas software; (E) precipitate size analysis with ImageJ software and the area where misorientation data was taken (red line) from Nanomegas ASTAR™ software; and (F) example of precipitate size analysis. (For interpretation of the references to colour in this figure legend, the reader is referred to the web version of this article.)

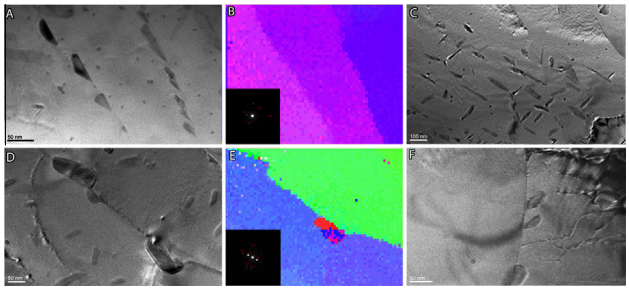

Figure 4. Examples of β phase after in situ heating experiments. (A) Growth on a 5° angle grain boundary. (B) Orientation map of (A) with an indexed diffraction of β phase precipitate. (C) β grown on dislocations in the matrix and (D) on a 40° angle grain boundary. (E) Orientation map of (D) with an indexed diffraction of β phase precipitate. (F) Dislocations leading to a β precipitate.

The grain boundary plane may also play a role in the formation and morphology of precipitates. This was found to be the case in the Davenport study [27], in which the susceptibility of a <20° higher-angle grain boundary was found to be more dependent on the grain boundary plane than on the misorientation between grains. It has been suggested that, for long-term sensitization, β phase grows preferentially on the {1 1 1} matrix with {1 1 2} as a secondary plane. This has an impact on how continuous the precipitate is along the grain boundaries [24,26]. Understanding the grain boundary plane and misorientation will lead to better understanding of the nucleation and formation of the β precipitates as a function of grain boundary free volume, which has been known to vary with grain boundary type [39]. Attaining information about the effect of the grain boundary plane will provide new insight into the initial β phase growth. Other factors, such as the percentage of Mg, have also been known to play a role, as some studies have shown that higher levels of Mg would lead to faster formation [24,30], which may explain the lack of growth at low-angle grain boundaries. This needs to be studied more extensively.

We have shown that initial β phase formation occurs on low-angle grain boundaries, which conflicts with previous observations of β phase growth only occurring on high-angle grain boundaries. Low-angle boundaries are susceptible to sensitization. Also, it has been shown that the β′ phase does not transform into β; rather, the β forms on its own after the β′ has begun to dissolve, which agrees with what has previously been suggested. The primary nucleation sites observed during in situ experiments are intergranular defects and low-angle subgrain boundaries. In many instances, the β phase formation preferred low-angle rather than high-angle grain boundaries. Although formation on low-angle boundaries was more prevalent, precipitate growth on low-angle boundaries was halted at a maximum size, most likely dependent on the boundary energy, whereas precipitates on high-angle boundaries show signs of uninhibited growth. Moreover, as the misorientation angle increased, the precipitate area also increased. Studies to better connect the dependence of β phase precipitation on both boundary structure and energy are underway.

The authors gratefully acknowledge funding from the Office of Naval Research under contract N000141210505.

Supplementary data associated with this article can be found, in the online version, at http://dx.doi.org/10.1016/j.scriptamat.2014.01.003.

[1] J.R. Davies, Corrosion of Aluminum and Aluminum Alloys, ASM International, Materials Park, OH, 1999.
[2] S. Lathabai, P.G. Lloyd, Acta Mater. 50 (2002) 4275.
[3] T. Lamb, N. Beavers, "The All Aluminum Naval Ship - The Way to Affordable Naval Ships", UK International Naval Engineering Conference and Exhibition, 2010.
[4] R.S. Yassar, D.P. Field, H. Weiland, Scr. Mater. 53 (2005) 299.
[5] R. Goswami, G. Spanos, P.S. Pao, R.L. Holtz, Mater. Sci. Eng. A. 527 (2010) 1089.
[6] I.N.A. Ogocha, O.J. Adigun, S. Yannacopoulos, J. Mater. Sci. 43 (2008) 4208.
[7] J.L. Searles, P.I. Gouma, R.G. Buchheit, Metal. Mater. Trans. A. 32A (2001) 2859.
[8] M.L.C. Lim, S. Jain, R.G. Kelley, J.R. Scully. In: Proceedings of the DoD Corrosion Conference, La Quinta, CA, 2011, http://nace.confex.com/nace/DoD2011/webprogram/Paper20419.html.
[9] M.C. Carroll, P.I. Gouma, M.J. Mills, G.S. Daehn, B.R. Dunbar, Scr. Mater. 42 (2000) 335.
[10] G.S. Frankel, N. Sridhar, Materials Today 11 (2008) 38–44.
[11] E. Bumiller, R.G. Kelly. In: Proceedings of the DoD Corrosion Conference, La Quinta, CA, 2011, http://nace.confex.com/nace/DoD2011/webprogram/Paper20366.html.
[12] C.B. Crane, R.P. Gangloff. In: Proceedings of the DoD Corrosion Conference, La Quinta, CA, 2011, http://nace.confex.com/nace/DoD2011/webprogram/Paper20175.html.
[13] P.G. Shewmon. New York: McGraw-Hill, 1963.
[14] M. Legros, G. Dehm, E. Arzt, T.J. Balk, Science 319 (2008) 1646–1649.
[15] F. Li, D. Xiang, Y. Qin, R.B. Pond Jr., K. Slusarski, Ultrasonics 51 (2001) 561.
[16] Y. Zhu, D.A. Cullen, S. Kar, M.L. Free, L.F. Allard, Metal. Mater. Trans. A. 43A (2012) 4933.
[17] R.L. Holtz, P.S. Pao, R.A. Bayles, T.M. Longazel, R.Goswami. In: Proceedings of the DoD Corrosion Conference, La Quinta, CA, 2011, http://nace.confex.com/nace/DoD2011/webprogram/Paper20421.html.
[18] L. Kramer, M. Phillippi, W.T. Tack, C. Wong, J. Mater. Eng. Perform. 21 (2012) 1025–1029.
[19] R.L. Holtz, P.S. Pao, R.A. Bayles, T.M. Longazel, R. Goswami, Metal. Mater. Trans. A. 43 (2012) 2839.
[20] M.J. Starink, A.M. Zahra, Acta Mater. 46 (1998) 3381.
[21] H. Yukawa, Y. Murata, M. Morinaga, Y. Takahashi, H. Yoshida, Acta, Metal. Mater. 43 (1995) 681.
[22] R. Goswami, R.L. Holtz, Metal Mater Trans A. 44 (2013) 1279–1289.
[23] L.L. Kaigorodova, Mater. Sci. forum. 294–296 (1999).
[24] Y. Yuan, University of Birmingham, PhD. Thesis, 2006.
[25] P.N.T. Unwin, R.B. Nicholson, Acta Metal. 17 (1969) 1379.
[26] L. Tan, T.R. Allen, Cor Sci. 52 (2010) 548.
[27] A.J. Davenport, Y. Yuan, R. Ambat, B.J. Connolly, M. Strangwood, A. Afseth, G. Scamans, Mater. Sci. Forum. 519 (2006) 641.
[28] E.F. Rauch, J. Portillo, S. Nicolopoulos, D. Bultreys, S. Rouvimov, P. Moeck, Crystallogr. Rep. 225 (2009) 103–109.
[29] J. Portillo, E.F. Rauch, S. Nicolopoulos, M. Gemmi, D. Bultreys, Mater. Sci. Forum. 644 (2010) 1–7.
[30] M. Popovic, E. Romhanji, Mater. Sci. Eng. A. 492 (2008) 460.
[31] S. Nebti, D. Hamana, G. Cizeron, Acta, Metal. Mater. 43 (1994) 3583.
[32] S. Lin, Z. Nie, H. Huang, B. Li, Mater Design 31 (2010) 1607.
[33] J.E. Hatch, Aluminum: Properties and Physical Metallurgy, ASM, Metals Park, OH, 1984.
[34] K. Unocic, PhD dissertation, The Ohio State University, 2008.
[35] D. Hamana, L. Baziz, M. Bouchear, Mater. Chem. Phys. 84 (2004) 112.
[36] M.D. Sangid, H. Sehitoglu, H.J. Maier, T. Niendorf, Mater. Sci. Eng. A. 527 (2010) 7115.
[37] J.A. Hren, G. Thomas, Trans. Metall. Soc. AIME 227 (1963) 308.
[38] G. Thomas, M.J. Whelan, Phil Mag. 6 (1961) 1103.
[39] G.J. Tucker, M.A. Tschopp, D.L. McDowell, Acta Mater. 58 (2010) 6464.